Periodica Polytechnica Civil Engineering, 66(4), pp. 1294–1308, 2022

Dynamic Response and Safety Control of Newly Poured Secondary Lining Concrete under Large Section Tunnel Blasting-A Case Study of Longnan Tunnel of Ganshen High-speed Railway

Linghao Xiong[1], Chuanbo Zhou[1*], Nan Jiang[1], Teng Wang[1], Xianzhong Meng[1]

[1] Faculty of Engineering, China University of Geosciences, No. 388 Lumo Road, Wuhan 430074, PR China
[*] Corresponding author, e-mail: cbzhou@cug.edu.cn

Received: 22 March 2022, Accepted: 31 August 2022, Published online: 14 September 2022

Abstract

The age of newly poured concrete is short, the cementation between aggregates is weak. At this time, the vibration will affect its performance. The secondary lining concrete newly poured in the tunnel is close to the work face and is susceptible to blasting vibration during construction. In order to study the safety threshold of blasting vibration velocity of newly poured secondary lining concrete in tunnels, the finite element model is established in ANSYS with the large-section Longnan tunnel project as an example. The attenuation law of vibration velocity in three directions of secondary lining under blasting load was analyzed by combining field blasting monitoring with numerical simulation, and the reliability of numerical simulation was verified. Through the numerical simulation results, the vibration velocity and von mises stress distribution of the newly poured secondary lining concrete of the tunnel are analyzed; combined with the dynamic tensile strength theory of concrete, the safety threshold of vibration velocity of newly poured secondary lining concrete of tunnel based on numerical calculation is established; through the indoor vibration test, taking the compressive strength and acoustic velocity of concrete as the indexes, the safety threshold of blasting vibration velocity of newly poured secondary lining concrete of tunnel based on shaking table test is obtained. Combined with the results of numerical simulation and vibration test, the safety threshold of blasting vibration velocity of newly poured secondary lining concrete in large-section tunnels is obtained, and the standard in this field is improved.

Keywords

blasting, tunnel secondary lining, newly poured concrete, dynamic response, safety threshold

1 Introduction

The safety and stability of secondary lining are very important for tunnel engineering, which should be controlled in construction. In recent years, with the rapid development of infrastructure construction in China, the technical and efficiency requirements of tunnel construction are also increasing. In order to shorten the construction period of some tunnels, blasting excavation and pouring secondary lining concrete are often carried out simultaneously. The age of the newly poured secondary lining concrete of the tunnel is short. At this time, the blasting vibration will have a series of effects on it, and even endanger the stability of the tunnel structure. Therefore, it is of great guiding significance to study the dynamic response characteristics and safety threshold of blasting vibration velocity of newly poured secondary lining concrete of large-section tunnels under blasting vibration.

Some scholars have conducted a lot of research on the influence of blasting vibration on tunnels. Monitoring detonation stress wave during blasting construction is the basic means to study this field. Wang et al. [1] monitored and analyzed the influence of blasting vibration on the new and old concrete lining during the tunnel expansion, and proposed the safety distance of concrete lining under blasting vibration. Different blasting hole types (cut hole, satellite hole and periphery hole) will cause different blasting vibration effects. Zhang et al. [2] and Xie [3] studied the influence of different blast hole types on tunnel lining structure through on-site monitoring. Deng et al. [4] and Krone [5] Studied the influence of explosion on the stability of tunnel structure by tunnel model test (the full-scale tests and the scaled-down tests).

Cite this article as: Xiong, L., Zhou, C., Jiang, N., Wang, T., Meng, X. "Dynamic Response and Safety Control of Newly Poured Secondary Lining Concrete under Large Section Tunnel Blasting-A Case Study of Longnan Tunnel of Ganshen High-speed Railway", Periodica Polytechnica Civil Engineering, 66(4), pp. 1294–1308, 2022. https://doi.org/10.3311/PPci.20206

With the rapid development of computer technology, many scholars use numerical simulation technology to simulate the dynamic response of tunnel structure under blasting. LS DYNA is a numerical simulation software based on nonlinear dynamic analysis, which is often used to simulate the blasting process. Most scholars use LS DYNA to study the influence of blasting vibration on the stability of tunnel secondary lining structure. Shao [6] and Jiang et al. [7] used LS-DYNA software to study the influence of tunnel cut hole blasting on the secondary lining of existing railway tunnels; Kong et al. [8] and Wang et al. [9] used LS-DYNA software to study the influence of explosion load on the lining structure of subway tunnel. Some scholars use the numerical simulation software LS-DYNA to study the influence of blasting vibration on different types of tunnel lining [10–15].

Using a single numerical simulation method to study the impact of blasting on tunnel secondary lining structure is lack of credibility. Therefore, the reliability of numerical simulation can be improved by combining field monitoring with numerical simulation. Yang et al. [16] studied the vibration characteristics of tunnel surface and surrounding rock by arranging vibration monitors on the rock surface and inside, and combining field monitoring and numerical simulation. Some researchers have studied the influence of short-range blasting on the existing tunnel lining by using the combination of field monitoring and numerical simulation [17–21]. Zhao et al. [22] studied the dynamic response of shotcrete at different ages under the coupling effect of explosion load and initial stress transient unloading of work face by using the comprehensive method of field monitoring and numerical simulation. Yang et al. [23] studied the blasting characteristics under high ground stress through field monitoring and numerical simulation, and evaluated the influence of blasting vibration on secondary shotcrete at different ages by using the maximum von mises stress criterion and Mohr-Coulomb criterion.

Blasting vibration will affect the reaction process of cement hydration, condensation and hardening in the new pouring concrete, which cannot be reflected in the numerical simulation. It is very necessary to carry out the vibration test of concrete in the laboratory to study the influence of explosion vibration on the performance of new pouring concrete. The compressive strength and acoustic wave velocity of concrete are two important indicators to measure the performance of concrete. Li et al. [24] applied impact load on different age concrete by drop hammer, analyzed the change of compressive strength of new concrete after impact damage. Hu [25] and He et al. [26] set four grades of newly poured concrete blocks at different blast standoff distances for blasting vibration test, and studied the influence of blasting vibration on the newly poured secondary lining concrete of tunnels with the acoustic damage degree of the vibrating concrete blocks as the index. Some scholars consider the dual indicators of compressive strength and acoustic wave velocity to study the impact of explosion vibration on the performance of new pouring concrete. Jin et al. [27] applied acceleration to concrete at different ages through indoor vibration test, and took compressive strength damage and acoustic wave velocity reduction as influence indexes to obtain the allowable vibration velocity of newly poured concrete. Wu et al. [28] used deep-hole blasting as the vibration source to test C40 concrete at different ages, and the allowable vibration velocity of C40 newly poured concrete was given with the reduction of compressive strength and acoustic wave velocity by 5% as the measurement index.

In the existing research, the research methods are generally one or two of the field monitoring, numerical simulation and vibration test, and the research method is relatively simple. Therefore, the combination of field test, numerical simulation and indoor vibration test to comprehensively analyze the research results is a reliable means to study this field.

This paper takes Ganzhou-Shenzhen high-speed railway longnan tunnel entrance section project as an example. The dynamic response characteristics and safety vibration velocity criterion of newly poured secondary lining concrete of tunnel under blasting vibration were studied by using three methods of field monitoring, numerical simulation and indoor vibration test. By means of field monitoring and numerical simulation results, the blasting dynamic response characteristics of concrete at different positions and ages of tunnel secondary lining are analyzed. Considering the dynamic ultimate tensile strength criterion of concrete, the safety threshold of blasting vibration velocity of new tunnel secondary lining concrete is proposed based on numerical simulation. Through the indoor vibration test, the vibration was applied to the secondary lining concrete block of the tunnel. After the maintenance was completed, the strength damage of the concrete block and the reduction law of acoustic wave velocity were analyzed. With 5% reduction rate as the measurement index, the safety vibration velocity threshold of blasting for newly poured secondary lining concrete of tunnel based on vibration test is proposed. Combined with the results of Safety regulations for blasting (AQSIQ and SAC, 2014) [29], numerical simulation and vibration test, the safety vibration velocity threshold of blasting for newly poured secondary lining concrete of large-section tunnel is finally obtained, which is used to guide the subsequent construction on site.

2 Project and vibration monitoring

2.1 Longnan tunnel project

Longnan Tunnel belongs to China's '13th Five-Year Key Project' Ganshen High-speed Railway Passenger Dedicated Line, located in Quannan County and Longnan County of Ganzhou City, Jiangxi Province(see Fig. 1). The length of the tunnel is 10.2 km from DK91+531 to DK101+775.27. Longnan tunnel adopts the form of single hole and double line, the net width is 14.4 m, the net height is 11.8 m, and the section area is 139.3 m^2, which is a super-long and super-large section tunnel. Longnan tunnel along the terrain, lithology is changeable, fault and groundwater development, blasting excavation in the process of roof collapse, gushing water and mud and other potential disasters, designed as a high-risk tunnel, is a key and difficult project in the construction of Jiangxi-Shenzhen high-speed railway.

The section studied in this paper is the entrance section of Longnan Tunnel with the mileage of DK91+920–DK92+260. The surrounding rock of the tunnel is mainly Yanshanian weakly weathered granite. The joint fissures are relatively developed, and the surrounding rock grade is III$_b$. The blasting excavation methods corresponding to different surrounding rock levels of Longnan Tunnel are also different. In order to control the half-borehole ratio of overbreak and underbreak and the wall of the tunnel, and improve the smooth blasting effect, the periphery holes are divided charging, connected with bamboo flakes and detonating cords, and strengthened charges are made at the bottom of the blast hole.

The cut hole and satellite hole are in the form of continuous charge, the non-electric nonel detonator is detonated backward, and all the borehole are blocked with stemming. The cut hole is arranged by two-stage compound angled cut, and the No.2 rock emulsion explosive with a diameter of 32 mm is used. The blasting excavation method is bench excavation, in which the upper bench height is 5.84 m, the lower bench height is 6.00 m, and the upper bench is 20 m ahead. The blasting parameters are set as shown in Table 1.

Table 1 Upper bench blasting parameters

Type	Quantity	Borehole length/m	Quantity of explosive rolls	Charge weight/kg
Cut hole	10	5.0	15	30
	8	5.0	15	24
Satellite hole	11	4.5	10–12	22–26.4
	12	4.0–4.5	10–12	22–26.4
	12	4.0–4.5	10–12	24–28.8
	15	4.0–4.5	8–10	24–30
Periphery hole	22	4.0	6	26.4
Bottom hole	13	4.0	6	15.6

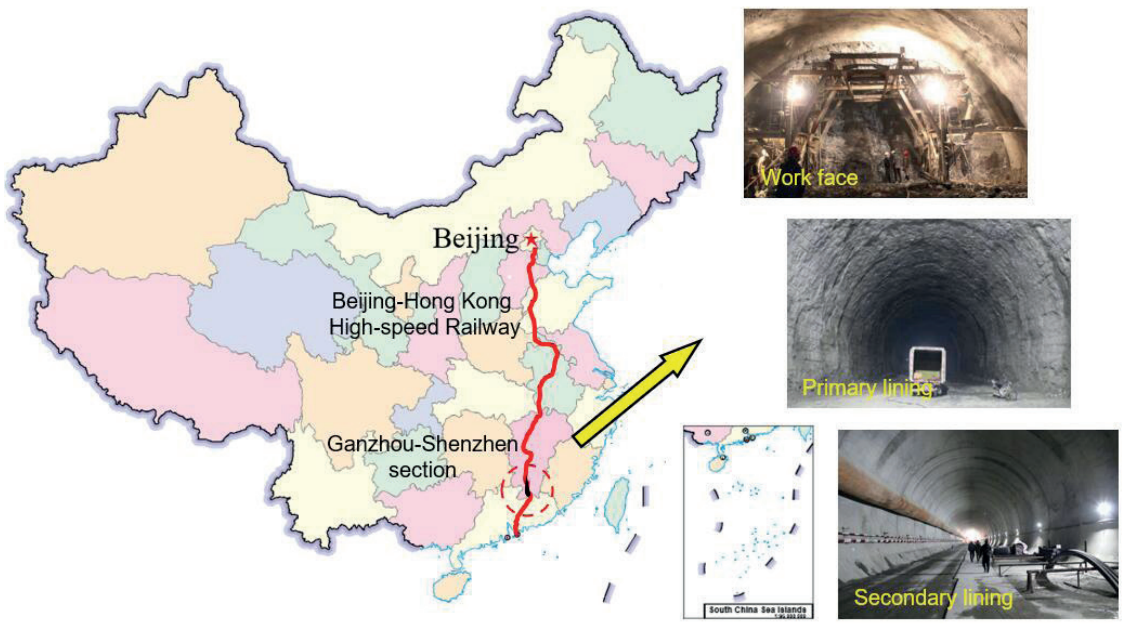

Fig. 1 Geographical location of Longnan Tunnel

2.2 Field blasting vibration monitoring

To study the dynamic response characteristics of newly poured secondary lining concrete under blasting vibration, 6 blasting vibration measuring instruments were arranged at the arch foot of the newly poured primary secondary lining in Longnan tunnel. The distance between 1# blasting vibration measuring instrument and blasting work face is 75 m, and each vibration measuring instrument is 2 m away. The position of the vibration measuring instrument is shown in Fig. 2.

The secondary lining concrete at the site blasting monitoring location is 1 day age, and Table 2 is the blasting data of 6 vibration measuring instruments. Select the blasting vibration waveform of the representative 1# blasting vibration measuring instrument, see Fig. 3.

Table 2 Data of blasting vibration measuring instrument

Number	Standoff distance (m)	Vibration frequency (Hz)			Peak vibration velocity(cm/s)		
		X	Y	Z	X	Y	Z
1	75	115.4	106.5	93.2	1.16	1.27	1.55
2	77	83.7	84.9	106.8	0.72	0.98	1.07
3	79	95.5	94.4	73.6	0.62	0.76	0.90
4	81	105.2	96.3	112.4	0.58	0.66	0.71
5	83	98.3	93.3	103.4	0.51	0.53	0.65
6	85	93.1	97.2	101.3	0.48	0.47	0.59

The frequency factor is taken into account in the vibration safety criterion in the Safety regulations for blasting. The allowable standard of blasting vibration safety for newly poured mass concrete is pointed out in the Safety regulations for blasting. It is required that the three components of particle vibration perpendicular to each other should be simultaneously measured in the blasting vibration monitoring. The particle vibration velocity is the maximum value of the three components, and the vibration frequency is the main vibration frequency. Usually, the main vibration frequency of blasting vibration generated by blasting construction is more than 100 Hz, which is far greater than the natural vibration frequency of tunnel structure.

The frequency factor is taken into account in the vibration safety criterion in the Safety regulations for blasting. The allowable standard of blasting vibration safety for newly poured mass concrete is pointed out in the Safety regulations for blasting. It is required that the three components of particle vibration perpendicular to each other should be simultaneously measured in the blasting vibration monitoring. The particle vibration velocity is the maximum value of the three components, and the vibration frequency is the main vibration frequency. Usually, the main vibration frequency of blasting vibration generated by blasting construction is more than 100 Hz, which is far greater than the natural vibration frequency of tunnel structure.

It can be seen from Table 2 that the main frequencies of blasting vibration in X, Y and Z directions are approximately close, which are far greater than the natural frequencies of the newly poured concrete structure with secondary lining. The blasting vibration velocity in X, Y and Z direction decreases with the increase of blasting standoff distance. The peak vibration velocities in X direction (tunnel transverse), Y direction (tunnel vertical) and Z direction (tunnel axial) are 1.16 cm/s, 1.27 cm/s and 1.55 cm/s, respectively. The peak vibration velocity in Z direction is larger than that in other directions, which needs to be controlled in construction.

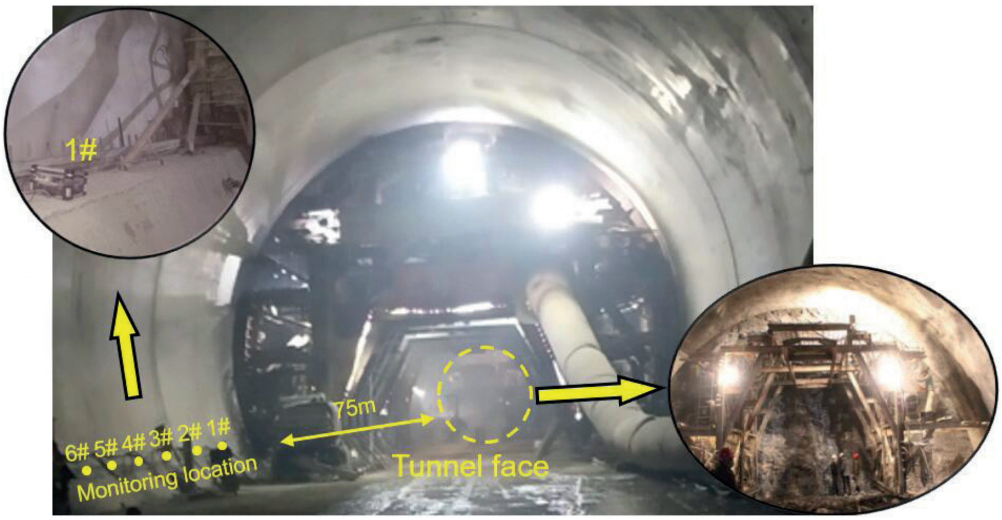

Fig. 2 Layout of monitoring points

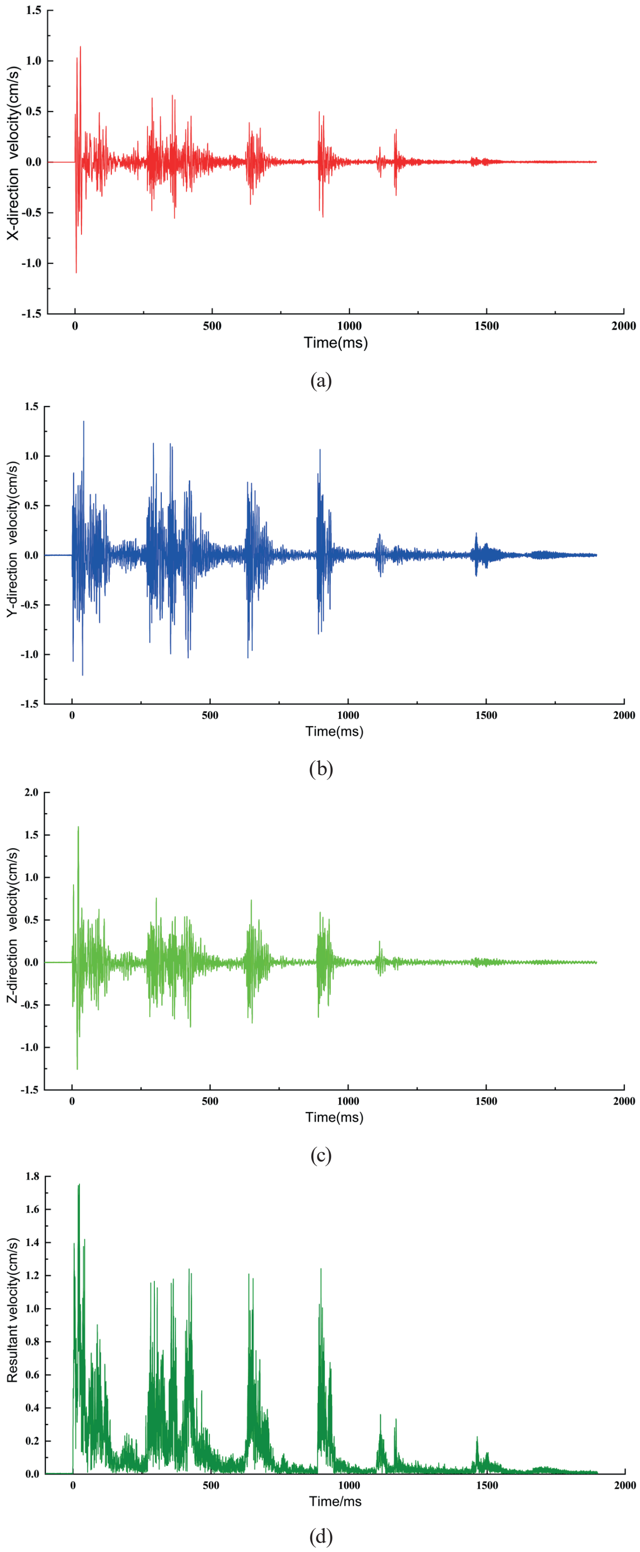

Fig. 3 1#Blasting vibration waveform of monitoring point (a) X-direction, (b) Y-direction, (c) Z-direction, (d) Resultant

It can be seen from Fig. 3 that multiple peaks and troughs can be clearly seen in the blasting vibration waveforms in X, Y and Z directions, and the peaks and troughs in three directions appear almost at the same time, and each band is relatively independent. This is because the millisecond delay detonator used in blasting is related, and different bands correspond to different segments of the detonator. Compared with the peaks and troughs at each time in Fig. 3, the peak vibration velocity in Z direction is usually significantly larger than that in X and Y directions, and the resultant vibration velocity after vector superposition is also close to the peak vibration velocity in Z direction. This shows that in the tunnel arch foot position, the peak vibration velocity in Z direction needs more attention. In the blasting vibration waveform diagram, the peak vibration velocity first appears, this is because the cutting hole with the largest single charge is first detonated, and the rock clamp is the largest at this time. There is only one free surface during cutting blasting, so the vibration is the largest.

3 Numerical model and verification

The effect of blasting vibration on the arch foot of new tunnel secondary lining was studied by field test. Since the blasting vibration measuring instrument can only be arranged on the ground, the vibration velocity at other positions of the secondary lining of the tunnel cannot be obtained. In order to study the response characteristics of the newly poured secondary lining concrete of the tunnel under the influence of blasting vibration, the numerical simulation software LS-DYNA was used for numerical simulation. By analyzing the distribution law of the peak particle velocity and von mises stress of the tunnel secondary lining concrete in the numerical simulation results, the safety threshold of the blasting vibration velocity of the newly poured tunnel secondary lining concrete based on numerical simulation is studied.

3.1 Equivalent explosion load

The field monitoring results show that the vibration load generated by the cut hole blasting is the largest. In order to simplify the calculation, the vibration generated by the cutting hole blasting is only considered in the numerical modeling. The blasting load generated by the cut hole is simplified as a triangular load and applied to the elastic equivalent boundary of the cutting hole. The influence of the load model on the blasting far area is similar to the actual field explosive blasting effect, and has high reliability.

For the simultaneous initiation of multiple cut holes, the explosion load equivalent to the elastic boundary is shown in Eq. (1) [30].

$$P_{be} = kP_0\left(\frac{r_b}{r_c}\right)^{2+\frac{\mu}{1-\mu}}\left(\frac{r_c}{r_f}\right)^{2-\frac{\mu}{1-\mu}} \quad (1)$$

Formula: k is the load influence coefficient of group-hole initiation, $k = 8–11$; P_0 is detonation pressure of explosives; r_b is charge radius; r_c is the radius of crushing zone, $r_c = 3–5\ r_b$; r_f is the radius of fracture zone, $r_f = 10–15\ r_b$; μ is Poisson's ratio of rock.

According to Eq. (1), the peak value of explosive load applied on the equivalent boundary is calculated, where the load rise time is 0.5 ms and the positive pressure action time is 5 ms [31]. The equivalent blasting load expression is shown in Eq. (2).

$$P_{be}(t) = \begin{cases} 13t, 0 \leqslant t < 0.5 \\ \dfrac{13(5-t)}{4}, 0.5 \leqslant t < 5 \\ 0, 5 \leqslant t \end{cases} \quad (2)$$

3.2 Numerical model and material

The finite element software ANSYS is used to establish the numerical model of the secondary lining of Longnan tunnel with large section. In order to save calculation time, the YOZ plane is taken as the symmetric plane to establish a 1/2 symmetric model. The overall size of the numerical model is 45 m × 100 m × 130 m (X × Y × Z), using 8-node SOLID164 element and cm-g-us unit system. To avoid the influence of reflection wave caused by artificial boundary on the calculation results, the five planes of the model are set as non-reflection boundary.

The tunnel span is 15 m and the height is 12 m. In the actual construction, the distance between the work face and the secondary lining is 75 m. The poured length of each formwork of the secondary lining is 12 m. The schematic diagram of the tunnel is shown in Fig. 4.

The elastic-plastic dynamic model of *MAT_PLASTIC_KINEMATIC is used for surrounding rock and secondary lining. This material model takes into account the elastic-plastic properties of rock medium materials, the effect of dynamic strengthening and strain rate variation. According to the mechanical test, the physical and mechanical parameters of Yanshanian granite are listed in Table 3.

The *JOHNSON_HOLMQUIST_CONCRETE constitutive model is used to define the primary lining concrete material, which is suitable for simulating the concrete material with large strain or under high pressure. The specific mechanical parameters of the primary lining are shown in Table 3.

For the elastic modulus of newly poured secondary lining concrete, The elastic modulus formula of concrete at different ages is shown in Eq. (3) [29].

$$E_c(t) = (0.7876 + 0.0095c) \times 28.8e^{-1.4171/t} \quad (3)$$

Formula: $E_c(t)$ is the elastic modulus of concrete at different ages; t is the age of concrete; c is the strength grade of concrete, $25 < c < 50$.

The tensile strength of newly poured secondary lining concrete was measured by indoor concrete splitting test, the tensile strength of concrete material determined

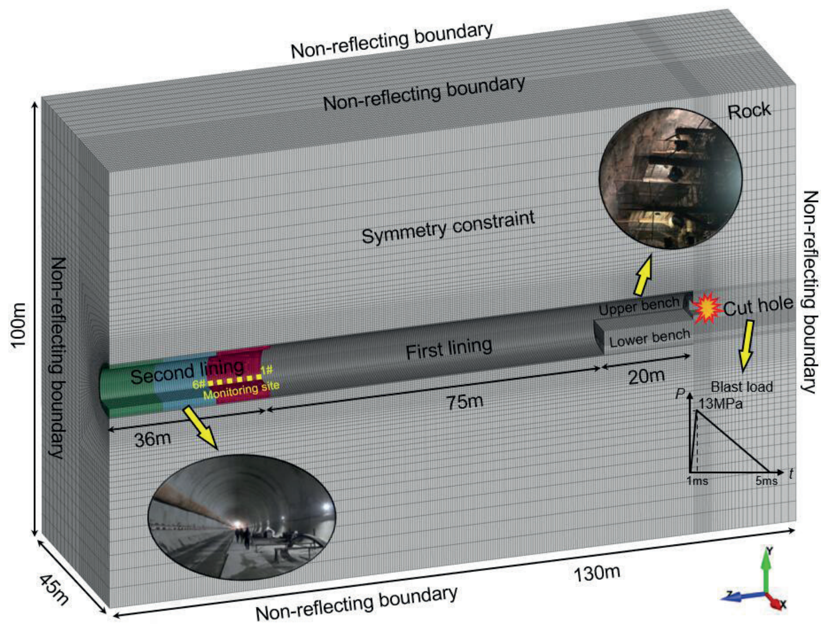

Fig. 4 Numerical model

Table 3 Mechanical parameters of rock and concrete

Material	Density/ (g·cm^{-3})	Elastic modulus/GPa	Poisson ratio	Tensile strength/MPa
Rock	2.30	40.00	0.31	5.50
Primary lining	2.60	23.00	0.19	3.30
1 day age concrete	2.60	7.49	0.19	1.10
2 day age concrete	2.60	15.21	0.19	1.31
3 day age concrete	2.60	19.26	0.19	1.54
5 day age concrete	2.60	23.27	0.19	1.67
28 day age concrete	2.60	30.00	0.19	2.23

by splitting test is static tensile strength, and the concrete physical and mechanical parameters of lining concrete are listed in Table 3.

3.3 Reliability verification

In order to verify the reliability of applying equivalent explosive load, the numerical model, meshing the model and selecting the material constitutive model, the elements of arch foot position corresponding to the field monitoring points in the numerical model are selected in turn. The element spacing is 2 m, and the distance between 1# monitoring point and work face is 75 m, as shown in Fig. 4.

The vibration velocities in X, Y and Z directions of the unit in the post-processing results are extracted and compared with the measured data of field blasting, as shown in Table 4.

The comparison between the measured blasting data and numerical simulation results in Table 4 shows that the error of simulation results is mostly controlled within 10%. It can be considered that the division of model grid, the application of equivalent load and the selection of material mechanical parameters in numerical simulation are reasonable, and the numerical simulation is reliable. At the same time, it can be seen that the simulated vibration velocity is larger than the measured data, which is because the numerical simulation modeling is simplified without considering the cracks and joints existing in the rock and soil itself, and the vibration velocity decays faster under the assumption of the ideality and isotropy of the material model.

4 Numerical simulations

4.1 Vibration response characteristics of secondary lining blasting in different positions of tunnel section

According to the field monitoring results, the blasting vibration velocity decreases with the increase of blasting standoff distance. To study the dynamic response characteristics of the newly poured secondary lining concrete at the arch of large-section tunnel under blasting load, the blasting vibration velocity and von mises stress of the arch of the 1-day-age numerical model are extracted and plotted on the tunnel section. The vibration velocity and von mises stress distribution characteristics of tunnel section are shown in Fig. 5.

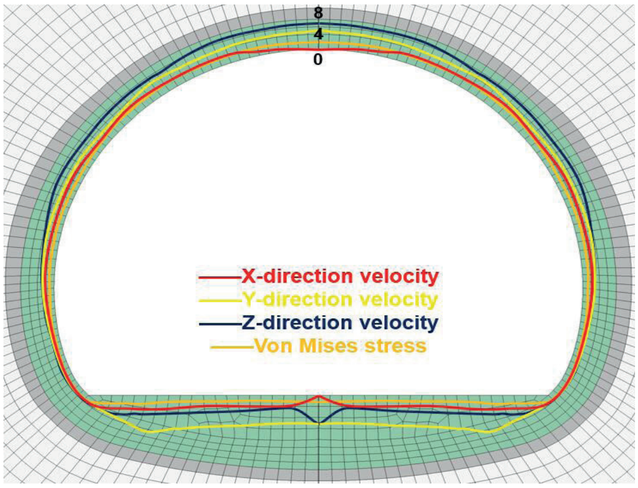

Fig. 5 Distribution of blasting vibration velocity and von mises stress

Table 4 Comparison of measured data and simulation results

Number	X-direction velocity (cm/s)		Error/%	Y-direction velocity (cm/s)		Error/%	Z-direction velocity (cm/s)		Error/%
	Monitor	Simulation		Monitor	Simulation		Monitor	Simulation	
1	1.16	1.10	5.45	1.27	1.35	6.30	1.55	1.68	8.39
2	0.72	0.77	6.94	0.98	1.09	11.22	1.07	1.20	12.15
3	0.62	0.71	14.52	0.76	0.84	10.52	0.90	0.98	8.89
4	0.58	0.63	8.62	0.66	0.73	10.61	0.71	0.76	7.04
5	0.51	0.55	7.84	0.53	0.57	7.55	0.65	0.72	10.77
6	0.48	0.51	6.3	0.47	0.51	8.51	0.59	0.65	10.17

It can be seen from Fig. 5 that under the blasting vibration load, the peak vibration velocity of the secondary lining arch at the 1st day of the tunnel is located at the vault, and the vibration velocity of the tunnel arch is mainly in the Z direction. The peak particle vibration velocity in X direction appears in the arch shoulder position, and the value is 1.98 cm/s. The particle vibration velocity in the vault and the middle of the bottom plate is small, which is related to the symmetry of the model. The X direction vibration velocity offsets each other at the position of the symmetric axis. The particle vibration velocity distribution in Y direction is close to circular, and the peak particle vibration velocity appears at the vault position, with a value of 4.65 cm/s. The Z direction is the axial direction of the tunnel, and the peak particle vibration velocity is 6.66 cm/s at the vault, which is related to the arrangement of the cutting holes in the upper step and the distance between the vault and the upper step. The peak von mises stress appears at the vault, which is1.57 MPa. In summary, the peak vibration velocity and peak von mises stress appear in the secondary lining vault, so the vault is the most dangerous position, which needs to be controlled in the process of blasting construction.

4.2 Vibration response characteristics of secondary lining blasting at different ages of tunnel arch

In order to analyze the dynamic response characteristics of secondary lining vault at different ages, the numerical models of 2 days, 3 days, 5 days and 28 days are established respectively, and the vibration velocity attenuation law of secondary lining concrete at different ages of large section tunnel vault is analyzed, as shown in Fig. 6.

From Fig. 6, it can be seen that the vibration velocity of the three directions of the secondary lining vault at different ages decreases exponentially with the gradual increase of the blast standoff distance. The particle peak vibration velocity appeared in the nearest position to the work surface (The standoff distance is 76 m), which was consistent with the results of blasting vibration monitoring at the construction site.

The particle vibration velocity in three directions decreases with the increase of concrete age at the same blast standoff distance, and the attenuation trend is slightly different. At the same blast standoff distance, in the X direction, with the increase of age, particle vibration velocity attenuation is accelerated; in the Y direction, with the increase of age, the attenuation of particle vibration velocity is small, and the attenuation law of particle vibration

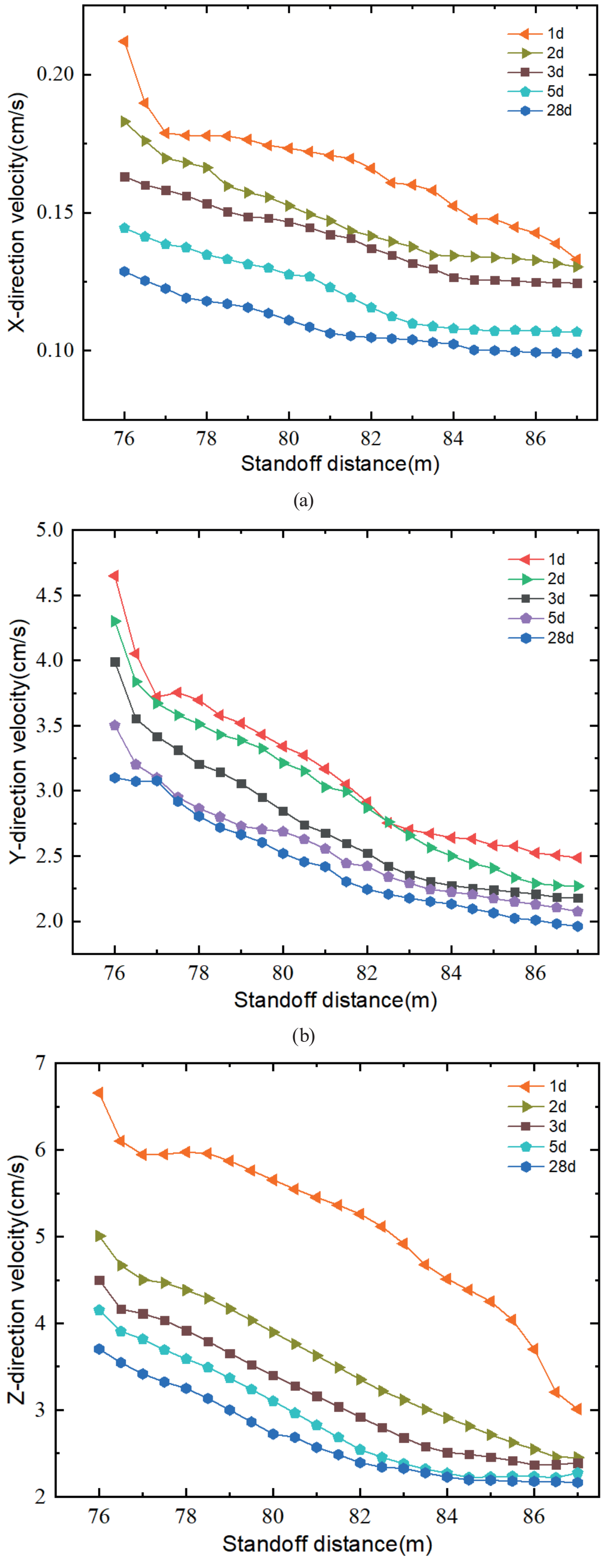

Fig. 6 Vibration Velocity Attenuation Diagram of Secondary Lining at Different Ages of Tunnel Arch (a) X-direction, (b) Y-direction, (c) Z-direction

velocity at different ages is close to the same; in the Z direction, the attenuation of particle vibration velocity slows down with the increase of age.

In summary, the vibration velocity in the Z direction of the secondary lining concrete at the arch top of the large-section tunnel at the age of one day is the largest, and the peak vibration velocity is 6.66 cm/s, which is much larger than that in other directions. This is because the hydration of the secondary lining concrete at 1-day age is not sufficient, and the cementation force between each aggregate is small, so the internal response of the concrete is large when subjected to blasting vibration. Therefore, the low-age secondary lining concrete is more prone to damage, which needs to be controlled in the blasting construction process.

4.3 Safety threshold analysis of blasting vibration velocity based on numerical simulation

According to the numerical simulation results, controlling the peak particle vibration velocity in the Z direction of the secondary lining vault of the large-section tunnel can ensure the safety of the newly poured secondary lining concrete of the tunnel. A series of elements of the vault position of the secondary lining of the tunnel at the ages of 1, 2 and 3 days are selected for analysis, and the specific values of vibration velocity and von mises stress in Z direction are counted, as shown in Fig. 7.

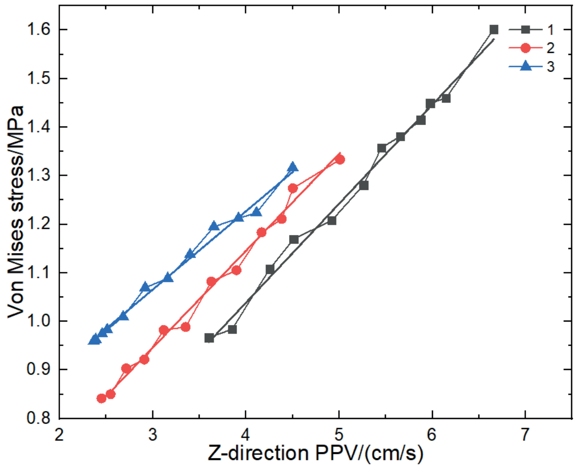

Fig. 7 Relationship between vibration velocity and von mises stress at the position of secondary lining vault

According to Fig. 7, the functional relationship between the von mises stress at the vault of the secondary lining of the tunnel at the age of 1, 2 and 3 days and the particle vibration velocity in the Z direction is shown in Eqs. (4)–(6).

$$\sigma_{t1} = 0.2038PPV + 0.2236 \quad (4)$$

$$\sigma_{t2} = 0.1962PPV + 0.3608 \quad (5)$$

$$\sigma_{t3} = 0.1927PPV + 0.3748 \quad (6)$$

Formula: σ_t is particle von mises stress, MPa; *PPV* is the peak particle vibration velocity, cm/s. When the concrete structure is damaged and cracked by blasting vibration load, its tensile strength shall adopt dynamic tensile strength. The relationship between dynamic tensile strength and static tensile strength of concrete is shown in Eq. (7) [7].

$$[\sigma_t] = \sigma_{t0}\left[1 + 0.12\lg\left(V_H\right)\right] = \overline{K_{DT}}\sigma_{t0} \quad (7)$$

Formula: $[\sigma_t]$ is dynamic tensile strength; $[\sigma_{t0}]$ is Static tensile strength; V_H is the loading rate, VH = σ_H/σ_1; σ_H is any load acceleration; σ_1 = 01 MPa; $\overline{K_{DT}}$ is the strength improvement factor, $\overline{K_{DT}}$ = 1.24–1.48.

The static tensile strength of concrete materials is measured by indoor concrete splitting test, as shown in Table 3. By substituting the static ultimate tensile strength into Eq. (7) to obtain the dynamic tensile strength of concrete, and then substituting the dynamic tensile strength into Eqs. (4)–(6), the peak particle vibration velocity of concrete under tensile failure according to the dynamic tensile strength theory can be obtained. According to the requirements of Code for design of railway tunnels (TB10003-2016) [32], the strength safety factor of 2.0 shall be taken for the concrete structure. Therefore, the allowable particle vibration velocity of tunnel secondary lining concrete at the age of 1–3 days is shown in Table 5.

In order to retain a certain safety margin, the dynamic tensile strength improvement factor K is taken as the small value of 1.24, and the safe vibration velocity of fresh concrete aged 1–3 days is 2.80–3.98 cm/s.

Table 5 Allowable particle vibration velocity of secondary lining concrete at different ages

Material	Static tensile strength (MPa)	Dynamic tensile strength (MPa)	Vibration velocity in case of damage (cm/s)	Safety factor	Vibration velocity threshold (cm/s)
1 day age concrete	1.1	1.36–1.63	5.59–7.00	2.0	2.80–3.50
2 day age concrete	1.31	1.62–1.94	6.42–8.05	2.0	3.209–4.025
3 day age concrete	1.54	1.91–2.28	7.97–9.89	2.0	3.983–4.944

5 Indoor vibration test

Because the blasting vibration will not only crack the concrete structure, but also reduce the cohesion between the aggregates in the newly poured concrete structure, and finally reduce the strength of the structure when the hydration reaction of the concrete structure is completed. Through the vibration test, the vibration load is applied to the concrete test block. Taking the strength damage of the concrete test block and the reduction of acoustic wave velocity as the standard, the influence of vibration velocity on the fresh concrete of different ages is studied. Finally, the safe vibration velocity threshold of newly poured secondary lining concrete of large section tunnel based on vibration test is proposed.

5.1 Vibration test design

In order to determine the vibration safety criterion of fresh concrete, the vibration frequency and vibration duration of secondary factors are taken as 60 Hz and 0.6 s. The influence of the main factors, namely the peak value of vibration velocity and the age of concrete, on the freshly poured concrete test block is analyzed. The values of each factor are shown in Table 6, and the blank group without vibration test is set.

The test adopts the cube concrete test block with side length of 100 mm. The mix proportion of concrete is the same as that of C30 concrete poured for the secondary lining at the construction site of the entrance section of Longnan tunnel, as shown in Table 7. After the test block is subjected to vibration load, it is placed in the standard constant temperature curing box for curing. When the curing reaches 28 days, its compressive strength and acoustic wave velocity are tested. To reduce the error, each group is set as 3 test blocks, and the test blocks are made at the same time.

Table 6 Values of various factors in vibration test

Number	Age (h)	Vibration velocity (cm/s)	Vibration frequency (Hz)	Time (s)
1	12	2.5	60	0.6
2	24	3.0	60	0.6
3	36	3.5	60	0.6
4	48	4.0	60	0.6
5	72	4.5	60	0.6

The effect of blasting stress wave on the far zone structure of tunnel can be simplified as sine wave. In this test, ZD/AB-ATP vibration instrument is used to load vertical sine wave on concrete test block to simulate blasting vibration, as shown in Fig. 8.

Install and fix the test block on the vibration instrument, and load the vertical sine wave on the concrete test block of different ages according to the test group designed in Table 6. After the test is completed, after demoulding, the test block shall be cured under standard conditions for 28 days, and the compressive strength test and acoustic wave velocity test shall be carried out, as shown in Fig. 9 and Fig. 10. When testing the acoustic velocity of concrete test block, use couplant to eliminate the influence of air between the probe and the test block, test the upper and lower, left and right, front and rear data of the test block and take the average value. Since the test block is a 100 mm cube, the average pressure value of each group of three test blocks is multiplied by 0.95 for the compressive strength test.

Fig. 8 ZD/AB-ATP vibration test instrument

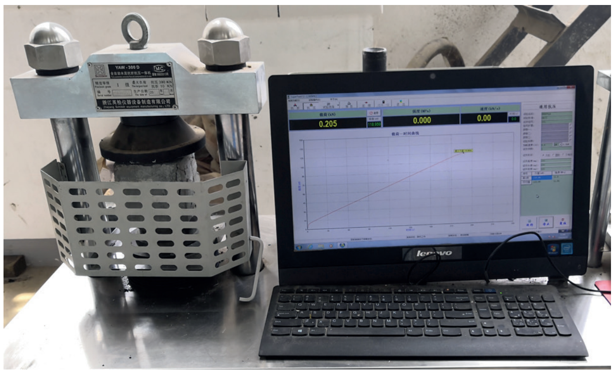

Fig. 9 Compressive strength test of test block

Table 7 Mix proportion of secondary lining concrete

425 portland cement	Fly ash	Medium sand	Small stone	Medium stone	Boulder	Water reducing agent	Water
1	0.25	2.44	0.70	1.76	1.05	0.01	0.54

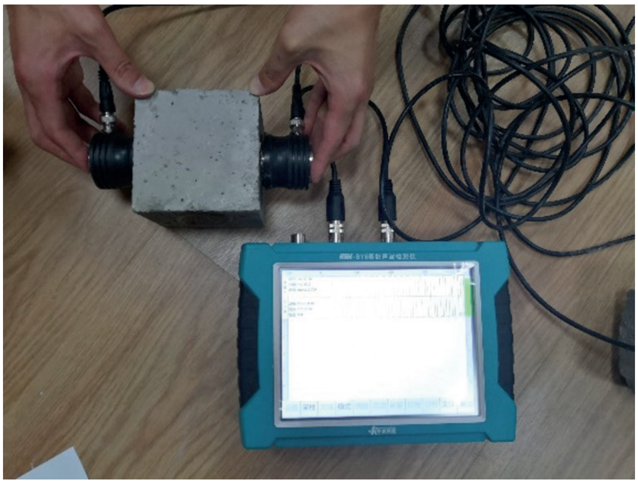

Fig. 10 Acoustic wave velocity test of test block

Compare the test group with the blank group without vibration test, and calculate the reduction rate of compressive strength and the damage rate of acoustic wave velocity. The reduction rate of compressive strength and the damage rate of acoustic wave velocity are calculated according to the following Eqs. (8) and (9).

5.2 Safety threshold analysis of blasting vibration velocity based on vibration test

Tables 8 and 9 are the test data of compressive strength and acoustic wave velocity of concrete test blocks after 28 days of curing.

Table 8 Compressive strength of concrete test block (MPa)

Velocity (cm/s) \ Age (h)	12 h	24 h	36 h	48 h	72 h
0	33.55	33.55	33.55	33.55	33.55
2.5	32.61	33.34	33.57	33.55	33.47
3.0	30.89	32.56	32.61	33.18	33.24
3.5	28.16	30.06	32.15	32.93	33.17
4.0	25.37	28.55	30.22	31.47	32.33
4.5	24.11	27.43	29.25	29.72	31.86

Table 9 Acoustic wave velocity of concrete test block (km/s)

Velocity (cm/s) \ Age (h)	12 h	24 h	36 h	48 h	72 h
0	4.235	4.235	4.235	4.235	4.235
2.5	4.129	4.167	4.192	4.166	4.183
3.0	4.082	4.102	4.137	4.153	4.161
3.5	3.935	3.977	4.035	4.134	4.149
4.0	3.739	3.842	3.827	4.027	4.137
4.5	3.473	3.566	3.799	3.935	4.066

Compare the test group with the blank group without vibration test, and calculate the reduction rate of compressive strength and the damage rate of acoustic wave velocity. The reduction rate of compressive strength and the damage rate of acoustic wave velocity are calculated according to the following Eqs. (8) and (9):

$$Z = 1 - \frac{P}{P_0} \quad (8)$$

Formula: P is the compressive strength of the test block of the test group after being subjected to vibration load; P_0 is the compressive strength of the control block not subjected to vibration load.

$$S = 1 - \frac{V_{pr}^{\ 2}}{V_p^2} \quad (9)$$

Formula: V_{pr} is the acoustic velocity of the test block of the test group after being subjected to vibration load; V_p is the acoustic velocity of the control block without vibration load.

Substitute the data in Table 8 and Table 9 into Eqs. (8) and (9) respectively to obtain the compressive strength and acoustic wave velocity attenuation diagram of the concrete specimen subjected to vibration, as shown in Fig. 11 and Fig. 12.

It can be seen from Table 8 and Fig. 11 that the shorter the age of concrete test block under vibration load, the greater the reduction rate of compressive strength after vibration load. Among them, the strength reduction of the test block at the age of 12 h increases rapidly with the increase of the peak value of vibration velocity. It shows

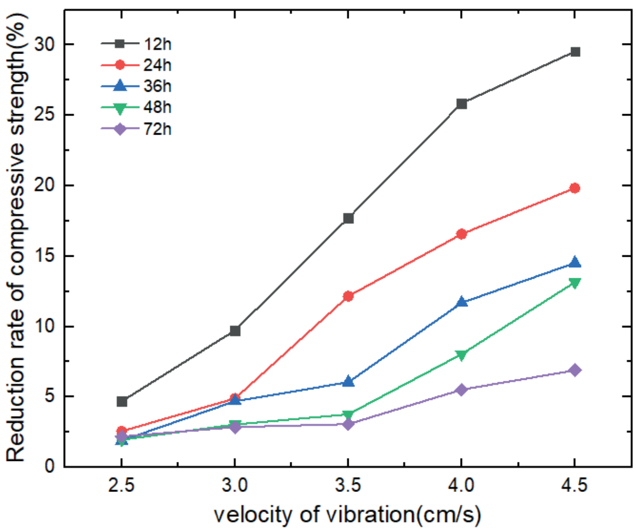

Fig. 11 Compressive strength attenuation

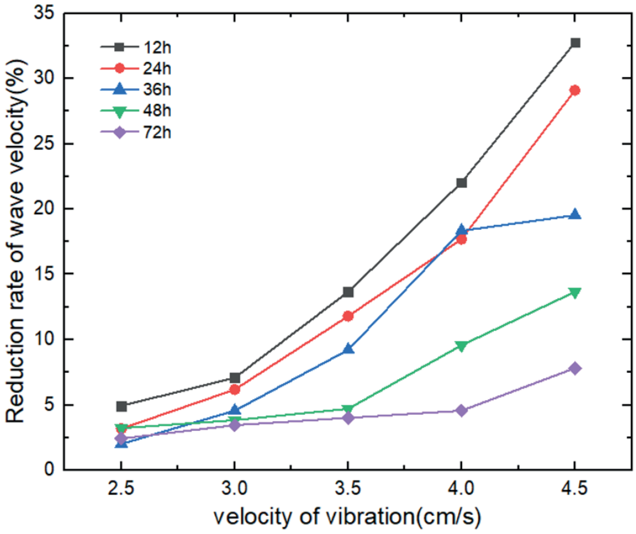

Fig. 12 Acoustic wave velocity attenuation

that the test block at the age of 12 h is most vulnerable to vibration load, and large damage will occur in it after bearing a certain strength of vibration. When the peak value of vibration velocity is less than 3.0 cm/s, the reduction rate of compressive strength is less than 6.18%, and then increases sharply with the increase of peak value of vibration velocity. The concrete at 24 h, 36 h, 48 h and 72 h age has a certain resistance to vibration load. When the peak vibration velocity is less than 3.0 cm/s, the strength reduction rate is less than 5%.

It can be seen from Table 9 and Fig. 12 that the shorter the age of concrete under vibration load, the greater the attenuation rate of sound wave velocity, which is the same as the reduction law of compressive strength. The 12 h and 24 h age curves are close, showing the law that the damage rate of sound wave velocity increases sharply with the increase of peak vibration velocity. It shows that there will be many micro cracks in the test block after the test block at the age of 12 h and 24 h is subjected to vibration load, which makes the sound wave velocity drop sharply and the damage degree of concrete rise sharply. The concrete aged 36 h, 48 h and 72 h has a certain resistance to vibration load. When the peak value of vibration velocity is less than 3.0 cm/s, the acoustic damage rate is less than 5%.

According to the above data and analysis, and combined with the current research status at home and abroad, the damage rate of compressive strength and the reduction rate of acoustic velocity are less than 5% as the safety judgment standard. The double evaluation standard based on the combination of compressive strength damage rate and acoustic velocity reduction rate is shown in Table 10.

6 Safety threshold of blasting vibration velocity of newly poured secondary lining concrete

The safe allowable vibration velocity obtained by comparing the Safety regulations for blasting, numerical simulation results and indoor vibration test is shown in Table 11.

It can be seen from Table 11 that the safety allowable standards obtained by numerical simulation and vibration test are basically the same. The results obtained by the two are slightly larger than those in the Safety regulations for blasting, because the secondary lining of Longnan tunnel adopts C30 concrete, while the Safety regulations for blasting is C20 concrete.

In addition, there are the following deficiencies in numerical simulation and vibration test:

(1) The reason why the numerical simulation results are too large is that in the process of establishing the numerical model, the surrounding rock and lining are isotropic materials, ignoring the anisotropy of surrounding rock and lining materials. The influence of joints and fissures on strength cannot be considered in numerical modeling, so the results may be larger than the actual results.

(2) The concrete test block is used in the vibration test. When the test block is subjected to vibration load, the test block has not been demoulded. The effect of size on the concrete pouring boundary is ignored. At the same time, the vibration test can only load the regular sine wave, which makes the test slightly different from the blasting vibration load in the actual construction.

By comprehensively comparing and analyzing the above two safe vibration velocitys, and referring to the tunnel blasting vibration control standard in the Safety

Table 10 safe vibration velocity of C30 concrete

Criteria	Vibration velocity (cm/s)				
Age (h)	12	24	36	48	72
The reduction rate of compressive strength ≤5%	2.5	3.0	3.0	3.5	3.5
The reduction rate of acoustic velocity ≤5%	2.5	2.5	3.0	3.5	4.0
result	2.5	2.5	3.0	3.5	3.5

Table 11 Safe vibration velocity of newly poured secondary lining concrete

Criteria	Vibration velocity (cm/s)				
Concrete age	12 h	1 d	36 h	2 d	3 d
Safety regulations for blasting			2.5–3.0		
Numerical simulation	/	2.8	/	3.2	4.0
Vibration test	2.5	2.5	3.0	3.5	3.5

regulations for blasting, the safety criterion of blasting vibration velocity of newly poured concrete for secondary lining of Longnan tunnel entrance section is put forward: When the concrete age is 1 day, the minimum safe vibration velocity is 2.5 cm/s; when the concrete age is 2 day, the minimum safe vibration velocity is 3.0cm/s; when the age of concrete is 3 days, the safe vibration velocitys obtained by numerical simulation and vibration test are 4.0 cm/s and 3.5 cm/s respectively, which is much larger than the safe vibration velocity specified in the code. Considering that the Safety regulations for blasting of newly poured concrete in the specification is C20, the safe vibration velocity threshold of 3 day age secondary lining concrete of Longnan tunnel can be set as 3.5 cm/s.

7 Conclusions

Based on the large section Longnan tunnel project, this paper adopts three research methods: on-site monitoring, numerical simulation and indoor vibration test. The dynamic response characteristics of concrete in different parts and ages of tunnel secondary lining under blasting vibration are analyzed. Combined with the results of numerical simulation and indoor vibration test, the safety threshold of blasting vibration velocity of newly poured secondary lining concrete of large section tunnel is determined. The main conclusions are as follows:

(1) According to the on-site blasting monitoring, the vibration velocities in X, Y and Z directions of the arch foot monitoring points of the secondary lining of Longnan tunnel decrease with the increase of the blasting standoff distance, and the vibration velocity in Z direction is greater than that in X and Y directions. The dominant frequencies of blasting vibration in the three directions are almost the same, which are far greater than the natural frequencies of the tunnel secondary lining and the newly poured concrete structure.

(2) Based on the numerical simulation results, the dynamic response characteristics of tunnel secondary lining fresh concrete under explosion load are as follows: The vibration velocity and von mises stress in the Z direction of the arch crown of the tunnel secondary lining at the age of 1 day are greater than those in other parts, and the peak vibration velocity and von mises stress appear in the arch crown, which are 6.66 cm/s and 1.57 mpa respectively; the vault of tunnel secondary lining is the most dangerous position, which should be controlled during blasting construction; the vibration velocity in three directions of tunnel secondary lining vault decreases exponentially with the increase of blasting standoff distance. The vibration velocity in three directions of tunnel secondary lining vault decreases with the increase of concrete age: At the same standoff distance, the attenuation of particle vibration velocity increases with the increase of age in the X direction; in the Y direction, the attenuation of particle vibration velocity is small with the increase of age, and the attenuation law of particle vibration velocity at different ages is close to the same; in the Z direction, the attenuation of particle vibration velocity slows down with the increase of age. Combining the numerical simulation results with the dynamic tensile strength theory and fully considering the strength reduction coefficient, the safe vibration velocity thresholds of tunnel secondary lining concrete blasting in 1, 2 and 3 days are 2.80 cm/s, 3.2 cm/s and 4.0 cm/s, respectively.

(3) Based on the indoor vibration test, the dynamic response characteristics of tunnel secondary lining fresh concrete under vibration load are as follows: With the increase of vibration velocity, the damage rate of compressive strength and the reduction rate of acoustic velocity of tunnel secondary lining concrete increase; under the same vibration velocity, the damage rate of compressive strength and the reduction rate of acoustic velocity of secondary lining concrete decrease with the increase of age; taking the damage rate of compressive strength and the reduction rate of acoustic velocity within 5% as the evaluation index, the safe vibration velocity thresholds of tunnel secondary lining concrete blasting at the age of 1, 2 and 3 days are 2.5 cm/s, 3.5 cm/s and 3.5 cm/s, respectively.

(4) Comparing the safe vibration velocity of Safety regulations for blasting, numerical simulation and vibration test, the safe vibration velocity thresholds of tunnel secondary lining concrete blasting in 1, 2 and 3 days are 2.5 cm/s, 3.0 cm/s and 3.5 cm/s, respectively.

Acknowledges

The author(s) disclosed receipt of the following financial support for the research, authorship, and/or publication of this article: The authors acknowledge the financial support from the National Natural Science Foundation of China (Grant No. 41972286).

References

[1] Wang, Y.-Q., Gong, L.-J., An, N.-N., Peng, X.-B., Wang, W., Wang, Z.-F. "Field Investigation of Blasting-Induced Vibration in Concrete Linings during Expansion of Old Highway Tunnel", Advances in Civil Engineering, 2021, 8820544, 2021. https://doi.org/10.1155/2021/8820544

[2] Zhang, Q., Li, L., Li, S., Ding, W., Hong, W. "Experimental study of blasting dynamic vibration of closely adjacent tunnels", Rock and Soil Mechanics, 29(10), pp. 2655–2660, 2008. (in Chinese) https://doi.org/10.16285/j.rsm.2008.10.012

[3] Xie, F. "Study on Vibration Effect of Blasting Inside the Construction Tunnel", PhD Thesis, China University of Mining and Technology, Beijing, 2017. (in Chinese) [online] Available at: https://kns.cnki.net/KCMS/detail/detail.aspx?dbname=CDFD-LAST2018&filename=1018051707.nh

[4] Deng, X., Wang, J., Wang, R., Liu, Q. "Influence of Blasting Vibrations Generated by Tunnel Construction on an Existing Road", International Journal of Civil Engineering, 18(12), pp. 1381–1393, 2020. https://doi.org/10.1007/s40999-020-00549-w

[5] Krone, E. "Internal Blast Loading of Submerged Floating Tunnels in Concrete", PhD Thesis, Norwegian University of Science and Technology, 2018.

[6] Shao, D. "Dynamic characteristics of newly-poured secondary lining in tunnel development blasting", Engineering Blasting, 23(03), pp. 47–51,72, 2017. (in Chinese) https://doi.org/10.3969/j.issn.1006-7051.2017.03.011

[7] Jiang, N., Zhou, C., Luo, G., Miao, G. "Blasting vibration safety criterion of railway tunnel concrete lining", Journal of Central South University (Science and Technology), 43(7), pp. 2746–2750, 2012. (in Chinese) [online] Available at: https://kns.cnki.net/kcms/detail/detail.aspx?dbcode=CJFD&dbname=CJFD2012&filename=ZNGD201207041&uniplatform=NZKPT&v=yrEgOE5UGQ4dHmOMl-nYbdccJKaudC3SHu1baY4tf7yV-C_DgbmIrviJwELs6mcz3

[8] Kong, D., Meng, Q., Zhang, W., Zhang, Q. "Shock responses of a metro tunnel subjected to explosive loads", Journal of Vibration and Shock, 31(12), pp. 68–72, 2012. (in Chinese) https://doi.org/10.13465/j.cnki.jvs.2012.12.003

[9] Wang, B., He, C., Xia, W. "Study on the interactive dynamic responses between the new-built subway tunnel by blasting construction and the existing operation subway tunnel", China Railway Science, 32(05), pp. 64–70, 2011. (in Chinese) [online] Available at: https://kns.cnki.net/kcms/detail/detail.aspx?dbcode=CJFD&dbname=CJFD2011&filename=ZGTK201105012&uniplatform=NZKPT&v=aIu5PqrXKUJ81H32Hj2groRjNvAgxURr_HFfEiOCfnlf7IA8ow79bfGsGlJmzc6t

[10] Wang, H., Liu, Z., Yang, C., Yang, T. "Three dimensional numerical analysis on damage of lining subjected to blasting loads during underground cavern enlarging", Journal of Vibration and Shock, (06), pp. 74–78+185, 2007. (in Chinese) https://doi.org/10.13465/j.cnki.jvs.2007.06.018

[11] Koneshwaran, S., Thambiratnam, D. P., Gallage, C. "Response of segmented bored transit tunnels to surface blast", Advances in Engineering Software, 89, pp. 77–89, 2015. https://doi.org/10.1016/j.advengsoft.2015.02.007

[12] Mussa, M. H., Mutalib, A. A., Hamid, R., Naidu, S. R., Mohd Radzi, N. A., Abedini, M. "Assessment of damage to an underground box tunnel by a surface explosion", Tunnelling and Underground Space Technology, 66, pp. 64–76, 2017. https://doi.org/10.1016/j.tust.2017.04.001

[13] Mussa, M. H., Mutalib, A. A., Hamid, R., Raman, S. N. "Blast damage assessment of symmetrical box-shaped underground tunnel according to peak particle velocity (PPV) and single degree of freedom (SDOF) criteria", Symmetry, 10(5), 158, 2018. https://doi.org/10.3390/sym10050158

[14] Yang, G., Wang, G., Lu, W., Yan, P., Chen, M. "Damage assessment and mitigation measures of underwater tunnel subjected to blast loads", Tunnelling and Underground Space Technology, 94, 103131, 2019. https://doi.org/10.1016/j.tust.2019.103131

[15] Tiwari, R., Chakraborty, T., Matsagar, V. "Dynamic analysis of twin tunnel subjected to internal blast loading", In: Matsagar, V. (ed.) Advances in Structural Engineering, Springer, 2015, pp. 343–354. ISBN 978-81-322-2189-0 https://doi.org/10.1007/978-81-322-2190-6_30

[16] Yang, J., Cai, J., Yao, C., Li, P., Jiang, Q., Zhou, C. "Comparative Study of Tunnel Blast-Induced Vibration on Tunnel Surfaces and Inside Surrounding Rock", Rock Mechanics and Rock Engineering, 52, pp. 4747–4761, 2019. https://doi.org/10.1007/s00603-019-01875-9

[17] Li, S., Yang, J., Xia, C., Zou, C. "Numerical simulation of close blasting on the impact of tunnel lining", Journal of China Coal Society, 36(S2), pp. 421–424, 2011. (in Chinese) https://doi.org/10.13225/j.cnki.jccs.2011.s2.015

[18] Zhao, H., Long, Y., Li, X., Lu, L. "Experimental and numerical investigation of the effect of blast-induced vibration from adjacent tunnel on existing tunnel", KSCE Journal of Civil Engineering, 20(1), pp. 431–439, 2016. https://doi.org/10.1007/s12205-015-0130-9

[19] Liang, Q., Li, J., Li, D., Ou, E. "Effect of Blast-Induced Vibration from New Railway Tunnel on Existing Adjacent Railway Tunnel in Xinjiang, China", Rock Mechanics and Rock Engineering, 46, pp. 19–39, 2013. https://doi.org/10.1007/s00603-012-0259-5

[20] Mobaraki, B., Vaghefi, M. "Numerical study of the depth and cross-sectional shape of tunnel under surface explosion", Tunnelling and Underground Space Technology, 47, pp. 114–122, 2015. https://doi.org/10.1016/j.tust.2015.01.003

[21] Liu, Z., Jiang, N., Sun, J., Xia, Y., Lyu, G. "Influence of tunnel blasting construction on adjacent highway tunnel: A case study in Wuhan, China", International Journal of Protective Structures, 11(3), pp. 283–303, 2019. https://doi.org/10.1177/2041419619888936

[22] Zhao, Z., Yang, J., Lu, W., Yan, P., Chen, M. "Selection of spraying time for permanent shotcrete in deep-buried tunnels based on evaluation of the influence of blasting vibration", Journal of Vibration and Shock, 34(07), pp. 8–14, 2015. (in Chinese) https://doi.org/10.13465/j.cnki.jvs.2015.07.002

[23] Yang, J. H., Lu, W. B., Zhao, Z. G., Yan, P., Chen, M. "Safety distance for secondary shotcrete subjected to blasting vibration in Jinping-II deep-buried tunnels", Tunnelling and Underground Space Technology, 43, pp. 123–132, 2014. https://doi.org/10.1016/j.tust.2014.04.008

[24] Li, Y., Gao, Z., Zhu, Q., Huang, X., Huang, X. "An experimental investigation into effects of blast-induced vibration on strength of early-age concrete", Explosion and Shock Waves, 3, pp. 22–27, 2013. (in Chinese). [online] Available at: https://kns.cnki.net/kcms/detail/detail.aspx?dbcode=CJFD&dbname=CJFD2013&filename=BZCJ201303003&uniplatform=NZKPT&v=vbQGBRr0eXMj672moCiy587R49IUZTiY5tc4HQcK3eMXfOgTIbaWRcysW5klMj5L

[25] Hu, J. "Influence of blasting vibration on newly poured ultra short age concrete secondary lining in mountain tunnel", Concrete, 9, pp. 149–152,160, 2021. (in Chinese) https://doi.org/10.3969/j.issn.1002-3550.2021.09.031

[26] He, Y., Chen, Q., Yi, L., Huang, X., Zeng, A., Zhou, X., Zhou, G. "Influence of tunnel blasting vibration on secondary lining of new ultra short age concrete", Journal of Central South University (Science and Technology), 51(02), pp. 507–513, 2020. (in Chinese) https://doi.org/10.11817/j.issn.1672-7207.2020.02.024

[27] Jin, Z., Yang, J., Ying, Y., Zhang, X., Zheng, S. "Experimental investigation on strength and damage of early-age concrete subjected to aftershock", Building Structure, 3, pp. 69–71, 2011. (in Chinese) https://doi.org/10.19701/j.jzjg.2011.03.016

[28] Wu, S., Wang, G., Yuan, D., Liu, D. "Experimental study on the influence of blasting vibration on fresh concrete", Journal of Vibration and Shock, 36(2), pp. 39–44, 2017. (in Chinese) https://doi.org/10.13465/j.cnki.jvs.2017.02.006

[29] Chinese Standard "GB6722-2014 Safety regulations for blasting", Standardization Administration of the People's Republic of China, Beijing, China, 2015. (in Chinese)

[30] Yang, J., Lu, W., Chen, M., Zhou, C. "An equivalent simulation method for blasting vibration of surrounding rock", Explosion and Shock Waves, 32(2), pp. 157–163, 2012. (in Chinese) [online] Available at: https://kns.cnki.net/kcms/detail/detail.aspx?dbcode=CJFD&dbname=CJFD2012&filename=BZCJ201202008&uniplatform=NZKPT&v=yR8Tdw1t6u24hW3SvD6xNWesZYzn32K6iT2NqL8JP_QQSFU7y6_tll2c1jT2ngGy

[31] Cheng, R., Chen, W., Hao, H., Li, J. "A state-of-the-art review of road tunnel subjected to blast loads", Tunnelling and Underground Space Technology, 112, 103911, 2021. https://doi.org/doi:10.1016/j.tust.2021.103911

[32] Chinese Standard "TB 10003—2016[S] Code for Design of Railway Tunnel", National Railway Administration of the People's Republic of China, Beijing, China, 2016. (in Chinese)